3B3-5

Near-Field to Far-Field Transformation Including the Effect of Ground Bounce

[#]Yoshio Inasawa, Shinji Kuroda, Kenichi Kakizaki,
Hitoshi Nishikawa, Naofumi Yoneda, Shigeru Makino
[1] Mitsubishi Electric Corporation
5-1-1 Ofuna, Kamakura-shi, Kanagawa, 247-8501, Japan, inasawa@ieee.org

1. Introduction

The far-field Radar Cross Section (RCS) measurement of the actual target requires a long measurement range, which can be realized in the outdoor site. One of the problems in outdoor measurement is the difficulty to avoid the effect of ground bounce. Some sites overcome the difficulty by the exploitation of the ground bounce in RCS measurement [1][2]. Meanwhile the RCS measurement of the large actual target in the far-field region is very difficult. The application of near-field to far-field RCS transformation method [3]-[5] is desired. However the non-uniformity of the illuminated electric field on the target causes some errors in the far-field RCS prediction. We propose a novel near-field to far-field RCS transformation method that is suitable for an outdoor RCS measurement. The validity of the proposed method is investigated by the simulation and measurement results.

2. Near-Field to Far-Field RCS Transformation for an Outdoor RCS Range

Figure 1 shows a scatterer located over the ground surface. The EM wave radiated from transmit antenna illuminates the scatterer via direct and reflected paths. There exist four multi-paths in consideration of transmit and receive antennas. The outdoor RCS range requires some conditions on the spatial relation. The antennas and scatterer to be measured must be set up so that the difference between direct and reflected path length becomes half wavelength. Furthermore it requires the small incident angle enough to yield the almost perfect reflection on the ground. The former condition is described by

$$H_a H_t = \frac{mR\lambda}{4}.$$

(1)

In general, the condition of m=1 is adopted. Under these conditions, the four components of scattered field can be considered to be almost same. The total received power will be 12dB stronger than if the scatterer were measured in a free space environment.

Figure 2 shows the coordinate system for RCS measurement on the ground plane. The target under test can be rotated in the Az(ϕ) and El(θ) direction. If the target were measured in the free space environment, the far-field RCS will be successfully predicted from measured electric field:Es(ϕ,θ) in the Fresnel region[3]-[5].

In case that the ground plane exists, the above procedures yield the prediction errors by the influence of ground bounce. The interference of a direct wave and reflected wave induces the nonuniform electric field distribution on the scatterer and it causes the error of far-field RCS prediction. We propose a novel algorithm that improves the prediction errors described above. The scattering coefficient is obtained by

$$Se(y, z) = \frac{4j\rho^2}{\lambda A(z)} \exp\left\{ jk\left(2\rho + \frac{y^2 + z^2 + H_a^2}{\rho}\right) \right\} \iint_{\vartheta y_w \phi_w} Es(\phi, \theta) \exp\left(-2jk\phi y - 2jk\theta z\right) d\phi d\theta$$

$$(2)$$

$$A(z) = -(e^{\frac{jkH_a \cos\alpha z}{\rho}} - De^{-\frac{jkH_a \cos\alpha z}{\rho}})^2$$
$$= -2\{1 + \cos(2kH_a \cos\alpha z / \rho)\} \quad (D = -1)$$

$$(3)$$

Here D is the reflection coefficient of the ground plane. The term A(z) represents the electric field distribution on the target. So A(z) becomes to be unity in the free space environment. Although the scattered fields include the effect of the electric field distribution on the target, the scattering coefficients in the free space are obtained by using Eq.(2). A(z) can correct the non-uniformity of the illuminated field distribution caused by the ground bounce. The far-field RCS is easily obtained by integrating the obtained scattering coefficient over the region of a target

$$\sigma = \frac{4\pi}{\lambda^2} \left| \iint Se(y, z) dy dz \right|^2.$$

$$(4)$$

3. Measurement and Simulation Result

We present the simulation and measurement results of the far-field RCS prediction from near-field data including the ground bounce. The near-field data is measured on the metal ground plane in an anechoic chamber, not on the actual ground plane, as shown in Fig.3 because the fundamental characteristics of ground bounce would be evident. The common specifications are shown in Table.1.

We show the predicted result from measured electric field data in the near-field region. The dimensions of measurement model shown in Fig.4 are 0.6m(Y) and 0.6m(Z). The measurement range of R=12m corresponds to 50% of the standard far-field condition ($= 2D^2/\lambda$) regarding both the horizontal and vertical dimensions. The far-field RCS predicted by the proposed method is shown in Fig.5. Here the far-field RCS is computed by equivalent edge current method[7]. Some errors are shown in the conventional method (w/o correction) by the non-uniformity of incident field on the target. Meanwhile the proposed method including a correction term A(z) successfully resolves the errors.

Figure 6 shows the computation model that is larger than the measurement model. The range of R=12m corresponds to 22% of the far-field condition. The effect of ground bounce would become clear. In Fig.7, the proposed method is also in good agreement with computed far-field RCS. Scattering coefficients obtained from around 0 degree data are shown in Fig.8. It is shown that the accuracy of scattering coefficients around the edge of the target is improved by the proposed method. The validity of the proposed method is demonstrated.

4. Conclusions

We presented the novel near-field to far-field RCS transformation method that can be applied for the outdoor RCS range. The simulation and measurement results are also presented. The validity of the proposed method is demonstrated.

References

[1] Nucholas C. Currie, Ed., "Techniques of Radar Reflectivity Measurement, " Chapter 8, Artech House, 1984.

[2] Rodger D. Nichols, Jon M. Stinson, Nancy E. Dougherty, James R. Newhouse, "ISO25/Z-540 Certification Activities at the Lockheed Helendale Outdoor RCS Range," Session 1-A064, pp.20-25, AMTA 2001.

[3] D. G. Falconer, "Extrapolation of near-field RCS measurements to the far zone, " IEEE Trans. Antennas Propagat., vol. 36, pp. 822 - 829, June 1988.

[4] Yoshio Inasawa, Hiroaki Miyashita, Isamu Chiba, Shigeru Makino, Shuuji Urasaki, "Far-Field RCS Prediction Method Using Cylindrical or Planar Near-Field RCS Data," IEICE Transactions on Electronics, Vol.E80-C, No.11, pp.1402-1406, November 1997.

[5] LaHaie, I.J., "Overview of an image-based technique for predicting far-field radar cross section from near-field measurements," IEEE Antennas and Propagation Magazine, Volume 45, Issue 6, pp.159-169, December. 2003.

[6] Yoshio Inasawa, Shinji Kuroda, Shinichi Morita, Hitoshi Nishikawa, Yoshihiko Konishi, Yonehiko Sunahara, and Shigeru Makino, "Far-Field RCS Prediction from Measured Near-Field Data Over Ground Plane," Proceedings of ISAP2005, Seoul, Korea, pp.601-604, August 2005.

[7] Yonehiko SUNAHARA, Hiroyuki OHMINE, Hiroshi AOKI, Takashi KATAGI, Tsutomu HASHIMOTO, "Separated Equivalent Edge Current Method for Calculating Scattering Cross Sections of Polyhedron Structures," IEICE Trans. Commun., Vol.E76-B, No.11, pp.1439-1444, 1993.
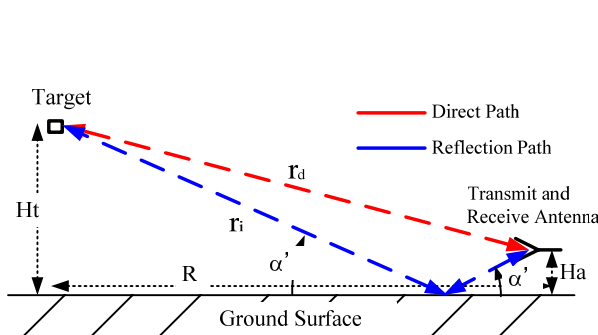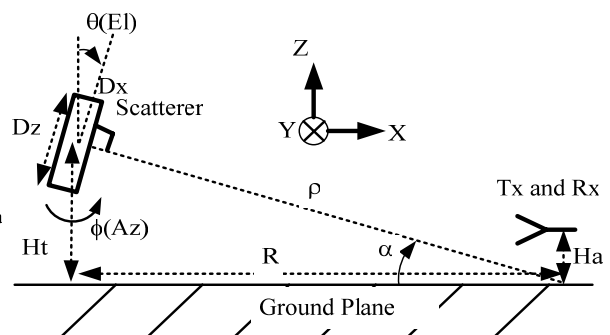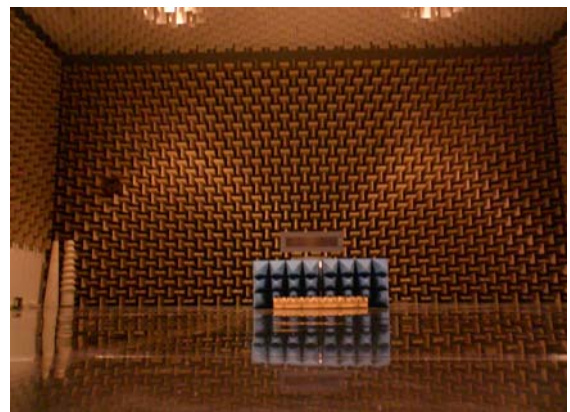
Figure 1:RCS Measurement over Ground Surface.

Figure 2:Coordinate System.

(a) Receive and Transmit Antennas.

(b)Measurement Model.

Figure.3:RCS Measurement Appearance.

Table 1:Measurement and Computation Specifications

Frequency	10.0GHz
Polalization	Horizontal
R	12.0m
Ha	0.1m (n=1)
Ht	0.9m

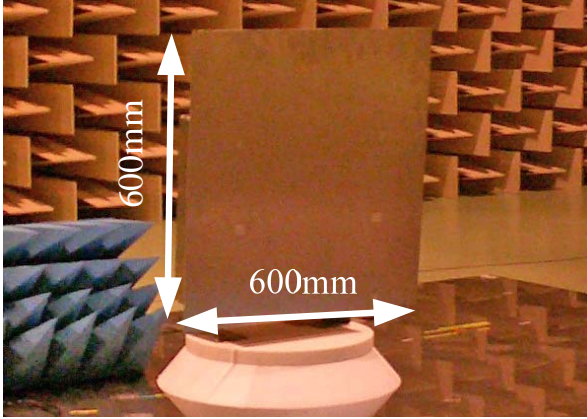
Figure 4:Measurement Model

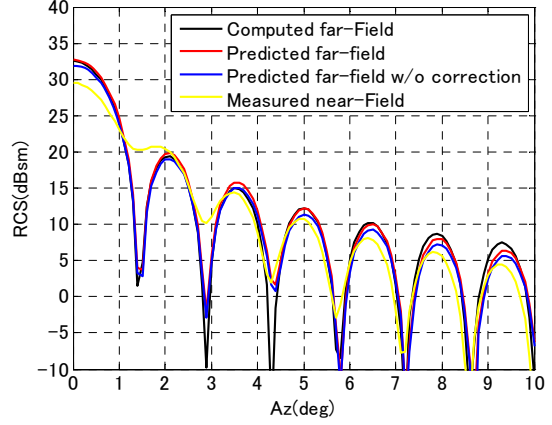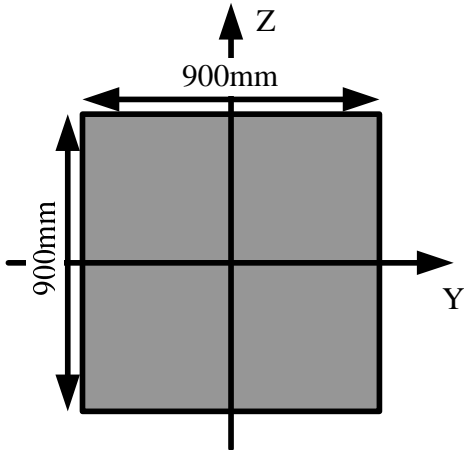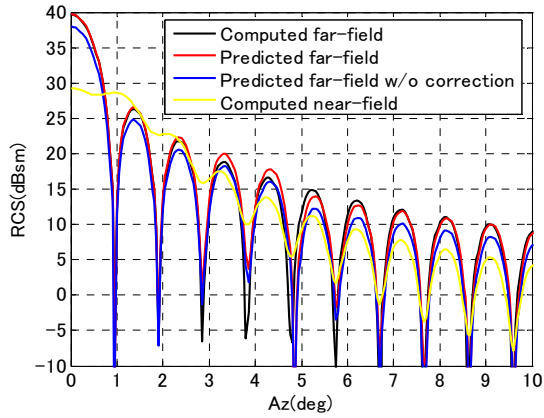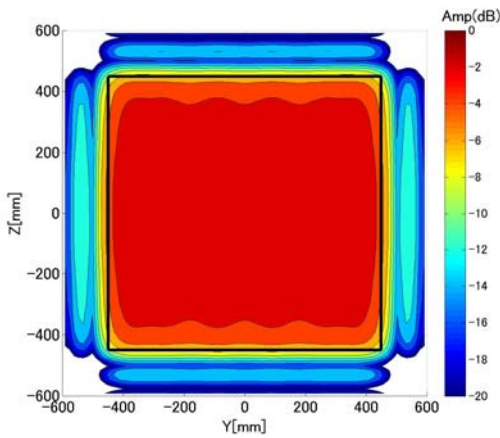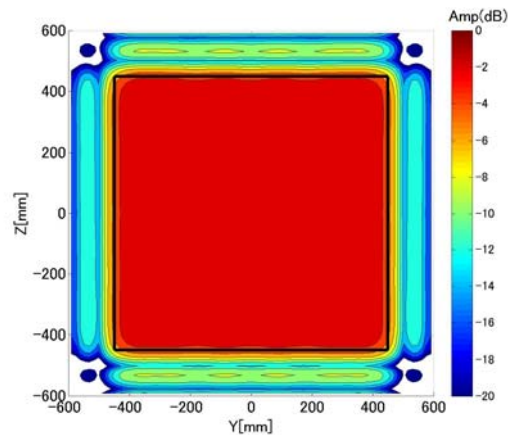Figure 5:Measured Result

Figure 6:Computation Model

Figure 7:Computed Result

(a)w/o correction

(b)w correction

Figure 8:Scattering Coefficients Obtained From Around 0 Degree Data